mathematics

MDPI

Article

Application of a Fuzzy Inference System for Optimization of an Amplifier Design

M. Isabel Dieste-Velasco

Electromechanical Engineering Department, Higher Polytechnic School, University of Burgos, 09006 Burgos, Spain; midieste@ubu.es

Abstract: Simulation programs are widely used in the design of analog electronic circuits to analyze their behavior and to predict the response of a circuit to variations in the circuit components. A fuzzy inference system (FIS) in combination with these simulation tools can be applied to identify both the main and interaction effects of circuit parameters on the response variables, which can help to optimize them. This paper describes an application of fuzzy inference systems to modeling the behavior of analog electronic circuits for further optimization. First, a Monte Carlo analysis, generated from the tolerances of the circuit components, is performed. Once the Monte Carlo results are obtained for each of the response variables, the fuzzy inference systems are generated and then optimized using a particle swarm optimization (PSO) algorithm. These fuzzy inference systems are used to determine the influence of the circuit components on the response variables and to select them to optimize the amplifier design. The methodology proposed in this study can be used as the basis for optimizing the design of similar analog electronic circuits.

Keywords: fuzzy systems; machine learning; applications; analog circuits; design

Citation: Dieste-Velasco, M.I. Application of a Fuzzy Inference System for Optimization of an Amplifier Design. *Mathematics* **2021**, *9*, 2168. https://doi.org/10.3390/math9172168

Academic Editors: Mario Versaci, Maria Paola Speciale and Alessandra Jannelli

Received: 19 July 2021
Accepted: 31 August 2021
Published: 5 September 2021

1. Introduction

Fuzzy inference systems (FISs) are powerful tools for analyzing the behavior of electronic circuits to optimize circuit design. They can be used for modeling the response of electronic circuit variables and to simultaneously identify the influence of circuit parameters on an output response. Circuit optimization presents some drawbacks due to the non-linearities in the components that affect the response. In addition, introducing tolerances into the components of the circuit affects the complexity of the resulting equations. Likewise, the use of optimization techniques without feedback from the design process can lead to impractical solutions because the optimized values may not be feasible due to the tolerances of some components and the instabilities that may be generated within the circuit. Therefore, the solution of the optimization process should be verified so that the circuit will remain stable despite any variations in the tolerances of the components.

In the present study, zero-order Sugeno fuzzy inference systems were used to optimize the design of a single stage of a small signal BJT amplifier. The response of this electronic circuit to variations that may arise from tolerances of the passive elements of the circuit were firstly obtained through a Monte Carlo analysis using Cadence®OrCAD® electronic simulation software. These obtained values were then used to build and train two zero-order Sugeno FISs in order to model both the voltage gain (Av) and the total harmonic distortion (THD), which, in itself, is complex to model analytically. The reduction in the THD is important and should be mentioned as it generates perturbations in the output voltage function. It is, therefore, of great technological interest to analyze its behavior in the design of analog circuits.

Any analytical determination of circuits with a high number of components is challenging due to both the existence of non-linearities and their complexity. Simulation together with fuzzy logic techniques can, therefore, contribute to adequately modeling

the aforementioned variables as well as to predicting their behavior and their interrelation with other response variables, in order to optimize the design of electronic circuits.

The methodology for optimizing the design of the electronic circuit proposed in this study shows that a fuzzy inference system may be trained to model the response variables of interest and, therefore, to acquire information on the circuit components and to determine their influence on the selected response variables. As shown below, in this study, an iterative process was used to optimize the circuit design using both simulation and FIS modeling.

The remainder of this paper is structured as follows: First a literature review of the state of the art related to this study is included in Section 2. Then, in Section 3, the methodology used to develop the fuzzy inference systems and to optimize the electronic circuit design is described. In Section 4, the results obtained both for the Av and for the THD are presented. A discussion of these obtained results is provided in Section 5. Finally, the main conclusions of this study are outlined in Section 6.

2. Literature Review

Mamdani [1] and Takagi–Sugeno [2] are the most commonly employed types of FIS for modelling circuit parameters. Several studies can be found in the literature dealing with the application of fuzzy systems [3,4]. Likewise, Oltean et al. [5] studied the application of various types of FISs both for modeling and designing electronic circuits; they proposed the application of a fuzzy optimization method to a CMOS operational amplifier. They employed an adaptive neuro-fuzzy inference system (ANFIS) to tune the initial zero-order Sugeno FIS. Sahu and Dutta [6] also employed fuzzy logic for the optimization of MOS operational amplifiers, and Hayati et al. [7] used a Takagi–Sugeno model and an ANFIS for modeling CMOS logic gates. In other studies, Hostos et al. [8] presented a design approach for active analog circuits using genetic algorithms, where the fitness function of the genetic algorithm is implemented by means of a fuzzy inference system; Wang et al. [9] designed integrated analog and radio frequency circuits. Regarding total harmonic distortion (THD) modeling, it is worth mentioning the studies of both Chang et al. [10], in which a FIS for shunt capacitor placement was employed in a distribution system considering harmonic distortions, and Panoiu et al. [11], in which an ANFIS was used for modeling the total harmonic distortion of the current and the voltage for a nonlinear high power load.

The use of fuzzy inference systems in electronic circuits for a faults' classification was examined by Arabi et al. [12], where an ANFIS is used to predict the faults in analog circuits. El-Gamal et al. [13] employed a fuzzy inference system for single analog fault diagnosis, and Kavithamani et al. [14] presented a fault detection algorithm based on SBT (Simulation Before Test) for verifying linear analog circuits by employing a fuzzy inference system as a classifier. They concluded that both single and multiple faults can be detected with their proposed method. Among many other studies, Ram et al. [15] applied a Mamdani FIS for the diagnosis of single and multiple faults in analog circuits, employing SBT approach.

Fuzzy inference systems are widely applied in several industrial areas, as they permit the efficient modeling of response variables. Among the studies that can be found in the relevant literature, Calcagno et al. [16] employed a Sugeno FIS to detect defects on thin metallic plates as a function of both their position and depth. Some other relevant studies are those of Guo et al. [17], who described the application of an ANFIS for partial discharge pattern recognition, and Voloşencu [18], who applied an ANFIS for the speed control systems of electric drives based on fuzzy PI controllers. Likewise, in another study, Napole et al. [19] employed fuzzy logic control to reduce the hysteresis effect and to increase the performance of piezoelectric actuators.

In other studies, Eboule et al. [20] compared artificial intelligent techniques and fuzzy logic to detect, classify, and locate faults on power transmission lines. Alhato et al. [21] employed an adaptive fuzzy extended state observer to improve the control performance of a DC-link voltage loop regulation in a double-fed induction generator-based wind energy converter.

Further examples of the industrial applications of fuzzy systems can be found in a study by Bagua et al. [22], where type-1 and type-2 fuzzy systems were used to monitor a gas turbine process or in a study by Angiulli et al. [23], who evaluated the resonant frequency of microstrip antennas. Likewise, the module faults in photovoltaic modules were characterized by Belaout et al. [24] and two ANFIS were used to detect photovoltaic system faults by Bendary et al. [25]. Finally, Chang et al. [26] studied laser module temperature control; many other research studies can be found in the literature in this field.

3. Methodology

As previously shown, fuzzy inference systems are commonly employed for modeling the behavior of electronic circuits and to detect and classify failures modes, among many other applications. In the present study, zero-order Sugeno fuzzy inference systems were used to optimize the design of a single stage of a small signal BJT amplifier. First, the response of the amplifier circuit versus variations that can arise from the tolerances of the passive elements of the circuit were obtained through a Monte Carlo analysis. Therefore, the resistive and capacitive components of the circuit varied as a function of their prescribed tolerances, from software simulations. As described below, the methodology proposed in this paper shows that a FIS may be trained to model the response variables of interest and, thereby, to acquire information on the circuit components and their influence on the selected response variables.

3.1. Initial Design

The electronic circuit analyzed in this study is depicted in Figure 1, showing an electrical diagram of a single stage of a small signal amplifier that was used as the circuit for modeling its behavior using two fuzzy inference systems. It is possible to use the proposed methodology for other types of analog circuits, either with more amplification stages or with a different configuration to the one shown in Figure 1.

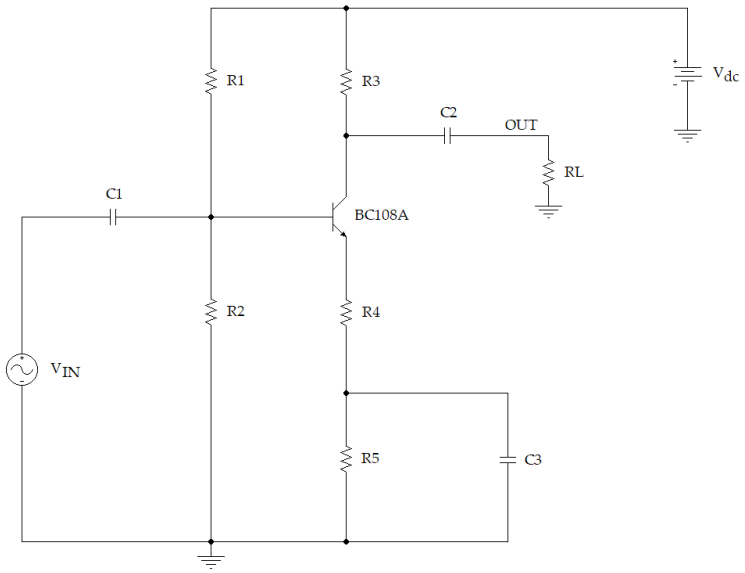

Figure 1. Electrical diagram of the single stage of a small signal BJT amplifier.

Table 1 shows the nominal values and the tolerances of the circuit components that were analyzed in this study. Table 2 shows the values of the power supply, the sinusoidal voltage source, and the load resistance. The amplifier circuit shown in Figure 1 was initially designed to operate in the active region. The output voltage of this circuit is shown in Figure 2.

Table 1. Nominal values and tolerances of the passive components of the circuit.

	R_1 (kΩ)	R_2 (kΩ)	R_3 (kΩ)	R_4 (kΩ)	R_5 (kΩ)	C_1 (μF)	C_2 (μF)	C_3 (μF)
Nominal value	15	2.7	5.6	0.1	1.8	100	10	47
Tolerance	10%	10%	10%	10%	10%	20%	20%	20%

Table 2. Values of the load resistance and the voltage sources of the circuit.

V_{IN} (Sinusoidal Voltage Source)	V_{dc} (Power Supply)	R_L (Load Resistance)
V_{INmax} = 10 mV; frequency = 1 kHz	20 V	8.2 kΩ

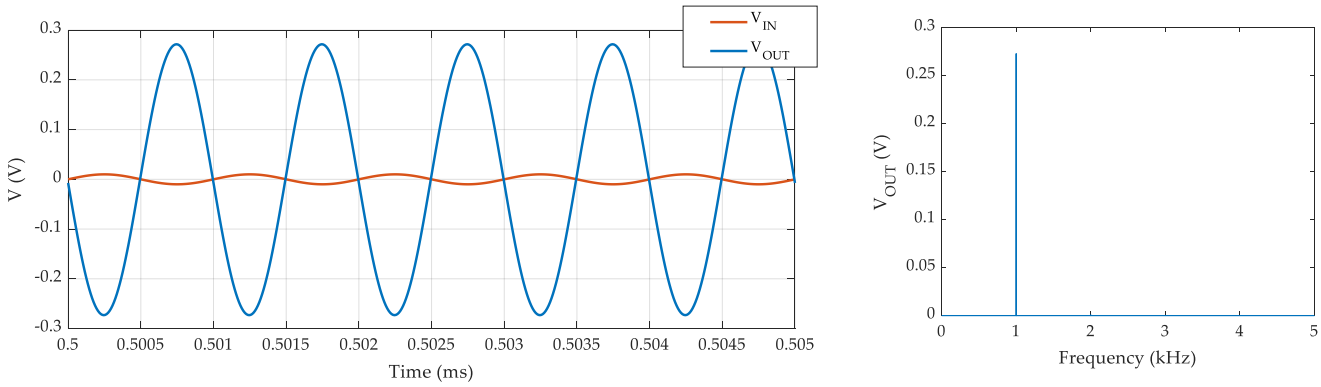

(**a**) (**b**)

Figure 2. (**a**) Input and output voltages; (**b**) FFT of the output signal.

As previously mentioned, the output variables are the amplifier voltage gain (Av) and the total harmonic distortion (THD (%)), which are determined from Equations (1) and (2), respectively. The THD (%) was defined from the voltage harmonics, as shown in Equation (2), where V_j is the Fourier component of the harmonic$_j$.

$$Av = \frac{\Delta V_{OUT}}{\Delta V_{IN}} \tag{1}$$

$$THD\ (\%) = 100 * \frac{\sqrt{\sum_{j=2}^{n} V_j^2}}{V_1} \tag{2}$$

Figure 2a shows both the output and the input voltage of the amplifier, and the fast Fourier transform (FFT) of the output signal is shown in Figure 2b. In this case, the amplifier voltage gain was Av = 27.2472 and the total harmonic distortion was THD = 0.2795% when the circuit was working with the nominal values of the components shown in Table 1.

However, the tolerances of the circuit components, as specified in Table 1, mean that the circuit may undergo variations in its output response, depending on the tolerance values, which, in turn, vary the circuit response. This behavior is represented in Figure 3, which shows the different voltage gain and harmonic distortion values from a Monte Carlo analysis of the designed circuit, with 128 runs, in which the passive elements of the circuit are varied within specified tolerances. The electronic simulation software employed in this study was Cadence®OrCAD®. Tables A1 and A2 in Appendix A show the values obtained from variations in the circuit components following the Monte Carlo analysis. In this study, uniform distributions were considered for the passive components of the circuit (resistors and capacitors). Then, the output values obtained in the amplifier circuit, shown

in Tables A1 and A2, were used to build and train the fuzzy inference systems in order to model both the gain voltage (Av) and the total harmonic distortion (THD) as a function of the electrical resistances and capacitors of the amplifier circuit.

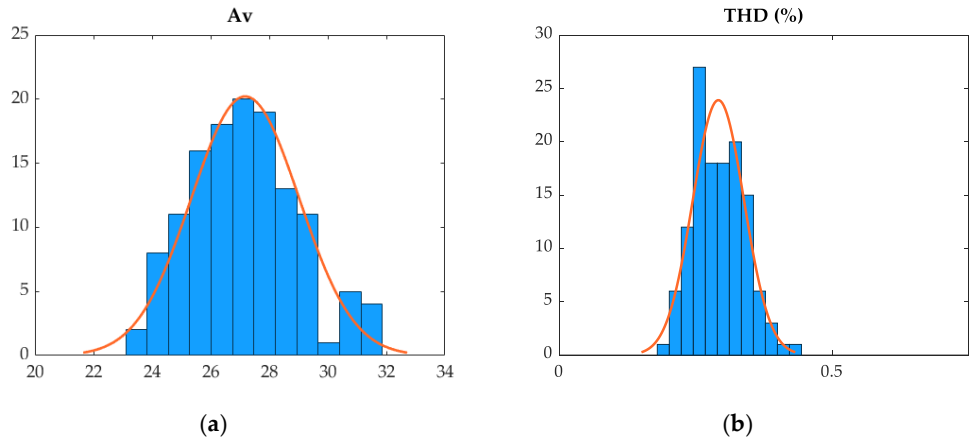

Figure 3. Histograms of the results with the initial design of the amplifier: (**a**) voltage gain (Av); (**b**) total harmonic distortion (THD).

Table 3 shows the average values and the standard deviations that were calculated from the results of the Monte Carlo analysis. These average values are close to those obtained with the nominal values of the initial configuration, which were Av = 27.2472 and THD = 0.2795%.

Table 3. Average and standard deviation values obtained from the Monte Carlo analysis in the initial design.

$\overline{\mathbf{Av}}$	$\mathbf{S_{Av}}$	$\overline{\mathbf{THD}}$ **(%)**	$\mathbf{S_{THD}}$ **(%)**
27.1805	1.8437	0.2918	0.0470

As shown in Table 1, the normalized components selected for the passive components of the amplifier circuit had tolerances of 10% in the case of the resistors and 20% in the case of the capacitors. The results from the Monte Carlo analysis were divided into two groups in order to train and then validate the fuzzy inference systems, as shown in Tables A1 and A2, respectively. The output of the initial design is shown in Figure 4 when the passive components of the circuit were varied in the Monte Carlo analysis.

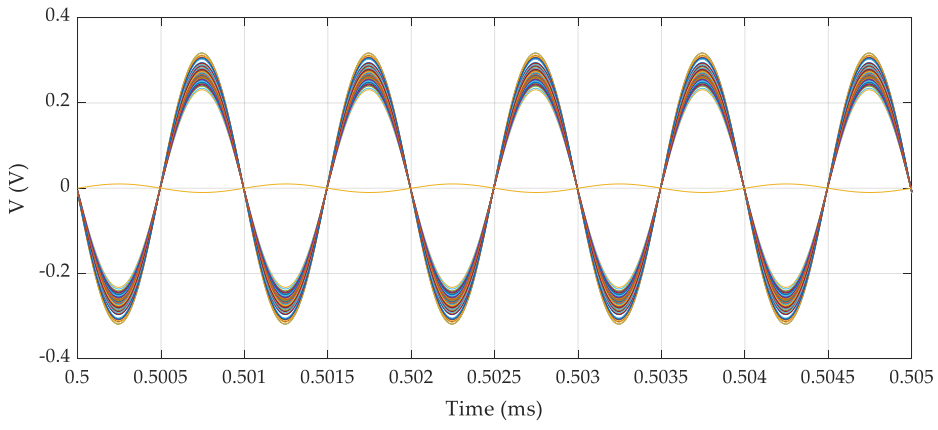

Figure 4. Response of the amplifier (Monte Carlo analysis).

3.2. Development of Fuzzy Inference Systems

Once the values of the Monte Carlo analysis were obtained, the Fuzzy Logic Toolbox of MATLAB™ 2020a [27] and the Global Optimization Toolbox of MATLAB™ 2020a [28] were employed to develop and tune the fuzzy inference systems so that the outputs of the circuit under study could be modeled, with the aim of analyzing the influence of the electrical components on both the voltage gain and the total harmonic distortion. The particle swarm optimization (PSO) algorithm of the Global Optimization Toolbox of MATLAB™ 2020a [28] was employed in the fuzzy inference systems developed in this study. The MATLAB™ defaults for the particle swarm optimization algorithm were used in this study. These values can be modified if necessary by setting the appropriate values in "options.MethodOptions". As shown in [28], this PSO algorithm is based on one proposed by Kennedy [29] and using modifications later suggested by Mezura-Montes et al. [30] and Pedersen [31]. In this algorithm, the objective function is evaluated at each particle location and the best values of both the function and the location are determined. Then, the algorithm is iteratively updated with these values until it reaches a stopping criterion [28]. Different descriptions of the PSO algorithm can be found in several papers, such as [32–34].

As shown in Figure 5, a zero-order Sugeno FIS was employed because the defuzzification process of a Sugeno FIS is computationally more efficient compared with that of a Mamdani FIS because, rather than evaluating the centroid, a Sugeno FIS evaluates a weighted average [27]. Two Gaussian membership functions were selected for the inputs (resistors and capacitors). In the fuzzy inference systems developed in this study, the fuzzy rules shown in Equation (3) were employed for both the Av and the THD, where the outputs (Av_j and THD_j) were constant values, as a zero-order Sugeno FIS was employed.

$$if\ (x_1\ is\ R_{1i})\ and\ (x_2\ is\ R_{2i})\ldots and\ (x_8\ is\ C_{3i})\ then \begin{Bmatrix} Av_j \\ THD_j \end{Bmatrix} = \begin{Bmatrix} k_{Av,j} \\ k_{THD,j} \end{Bmatrix} \tag{3}$$

where $j = 1 \ldots n$ and n is the number of $if - then$ rules; and Av_j and THD_j are the outputs of the jth $if - then$ rule. Therefore, given a specific input, the outputs of the fuzzy model (Av and THD) may be obtained from Equations (4) and (5), respectively.

$$Av = \frac{\sum_{j=1}^{n} \omega_j * Av_j}{\sum_{j=1}^{n} \omega_j} \tag{4}$$

$$THD = \frac{\sum_{j=1}^{n} \omega_j * THD_j}{\sum_{j=1}^{n}{}_j} \tag{5}$$

where ω_j, the weight of the jth $if - then$ rule for a specific input vector, is evaluated, as shown in Equation (6), for both Av and THD. It can be observed that $m = 8$ because eight inputs (five resistors and three capacitors) exist and $F_{jk}(x_k)$ is the membership grade of x_k in F_{jk}.

$$\omega_j = AndMethod\left\{F_{jk}(x_k)\right\} = \prod_{k=1}^{m=8} F_{jk}(x_k) \tag{6}$$

As previously mentioned, a Monte Carlo analysis was first performed to obtain the amplifier circuit response. Figure 6 shows the variation in the passive components of the circuit depicted in Figure 1 after considering a uniform distribution for these components.

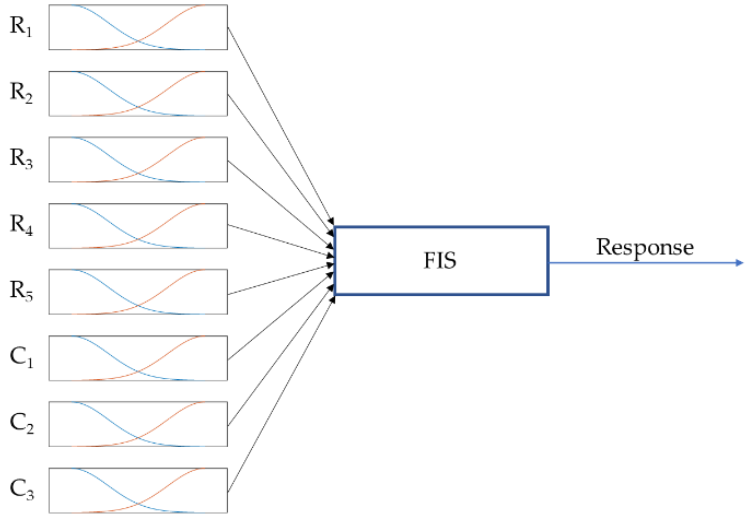

Figure 5. Zero-order Sugeno FIS.

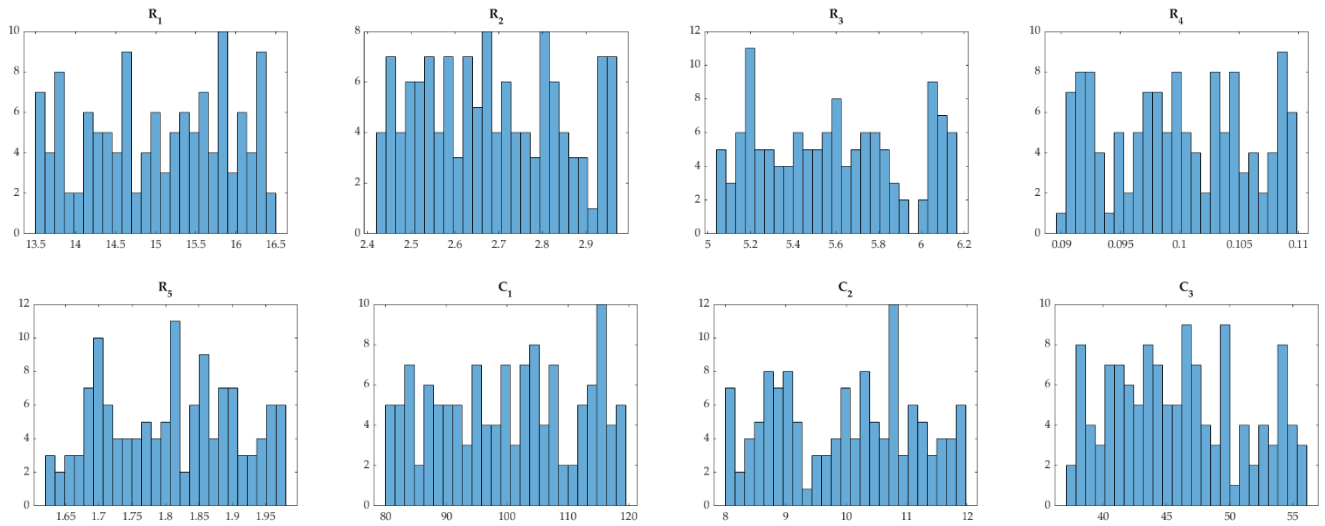

Figure 6. Histograms showing the values employed in the Monte Carlo Analysis (grouped in 25 bins).

The data obtained from the Monte Carlo analysis were divided into two subsets of the same size: one to train the fuzzy inference systems and another to validate them, as shown in Tables A1 and A2, respectively. Therefore, a FIS was first developed from the input and output variables of the circuit. With this objective in mind, the "addInput/addOutput" options of MATLAB^{TM} were used. Two untuned fuzzy inference systems (one for the Av and one for the THD) were developed using Gaussian-type membership functions for both the Av and the THD, respectively. The software was set to automatically select the values of the constants of the membership functions. Any other criterion could have been used to develop the initial FIS, but the former was chosen to simplify the process. Furthermore, to develop these two initial untuned zero-order Sugeno fuzzy inference systems, it was decided to use a maximum number of membership functions for the response (the Av and the THD) equal to the length of the response vector obtained from the Monte Carlo analysis and divided by two. A different number of membership functions could have been selected for the output, but it was decided to use this number of outputs, which, in this case, amounted to 32 membership functions. Likewise, to obtain the initial FIS, the range of variation in the variables was determined from the Monte Carlo analysis, multiplying these ranges of variation, of inputs and outputs by a k factor to expand the range of variation. In

the case in this study, a factor of k = 0.5 was considered. That is, the range of variation was [nominal*(1 − k), nominal*(1 + k)].

Figure 7 shows the membership functions that were generated in the untuned fuzzy inference systems. Once these zero-order Sugeno fuzzy inference systems were developed, they were tuned in two steps, following the methodology shown in the Fuzzy Logic Toolbox of MATLAB^{TM} 2020a [27]. Therefore, the PSO optimization algorithm "particleswarm" was used first, along with the optimization type set to "learning" to generate the rules of the FISs because the initial FISs were untuned. In this first step, 25 iterations were selected.

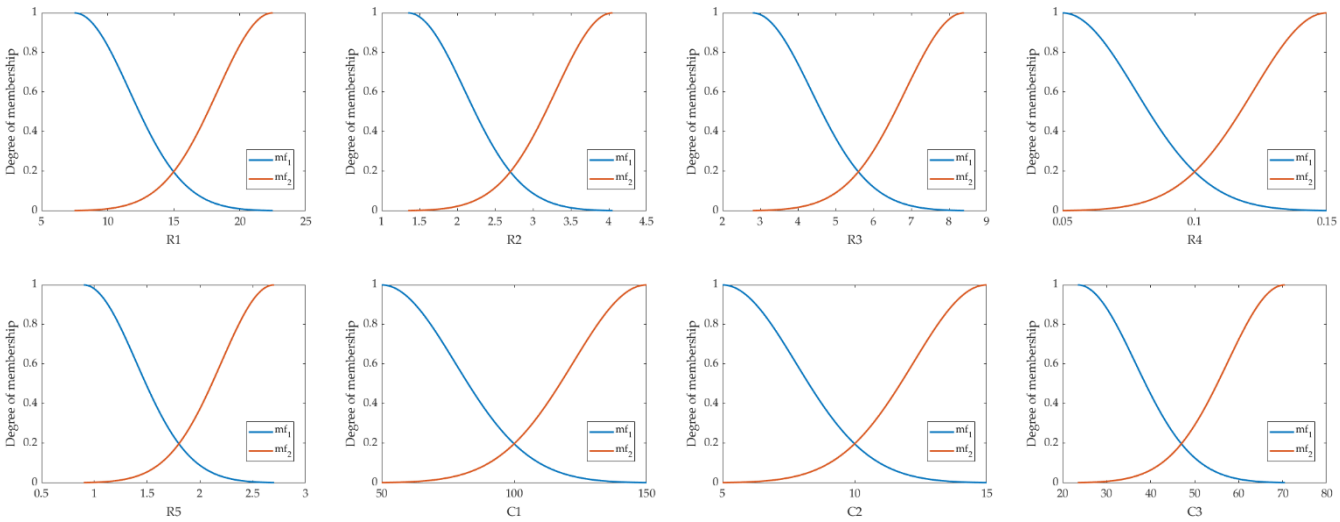

Figure 7. Membership functions employed for Av and for THD before tuning the Fuzzy Inference Systems.

3.3. Tuning of the Fuzzy Inference Systems

Once these fuzzy inference systems were generated for both the Av and the THD, in a second step, the membership function and the learning rules of each FIS were tuned. In this second case, 100 iterations were performed by using the "tuning" option in MATLAB^{TM}, once again with a PSO optimization algorithm, although any other method could have been employed [27].

Figures 8 and 9 show the tuned membership functions of each FIS. The FIS models obtained in this way were employed for modeling the behavior of the amplifier circuit.

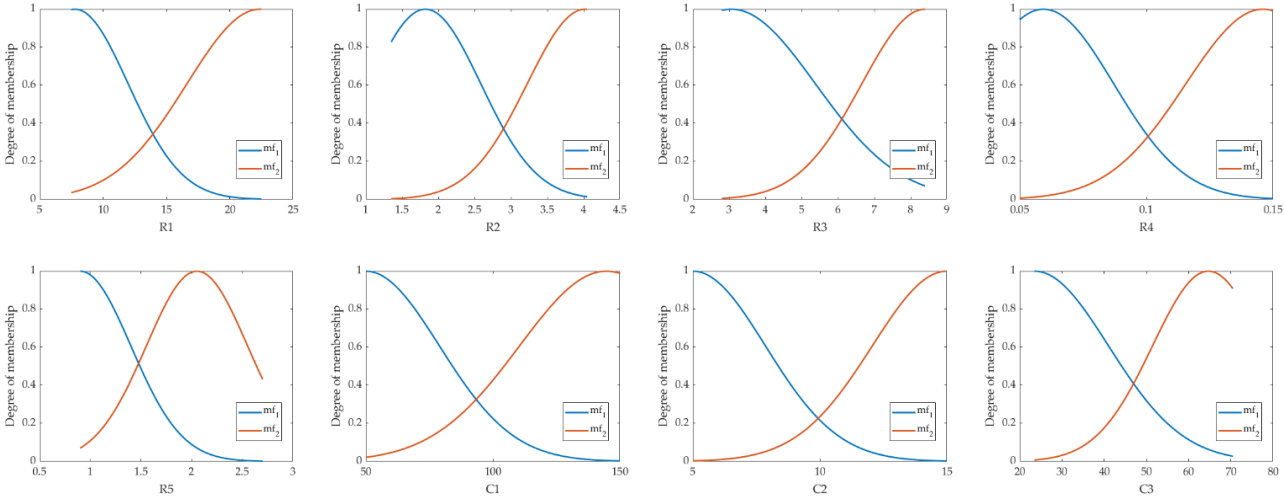

Figure 8. Membership functions obtained after tuning the FIS for Av (2nd step).

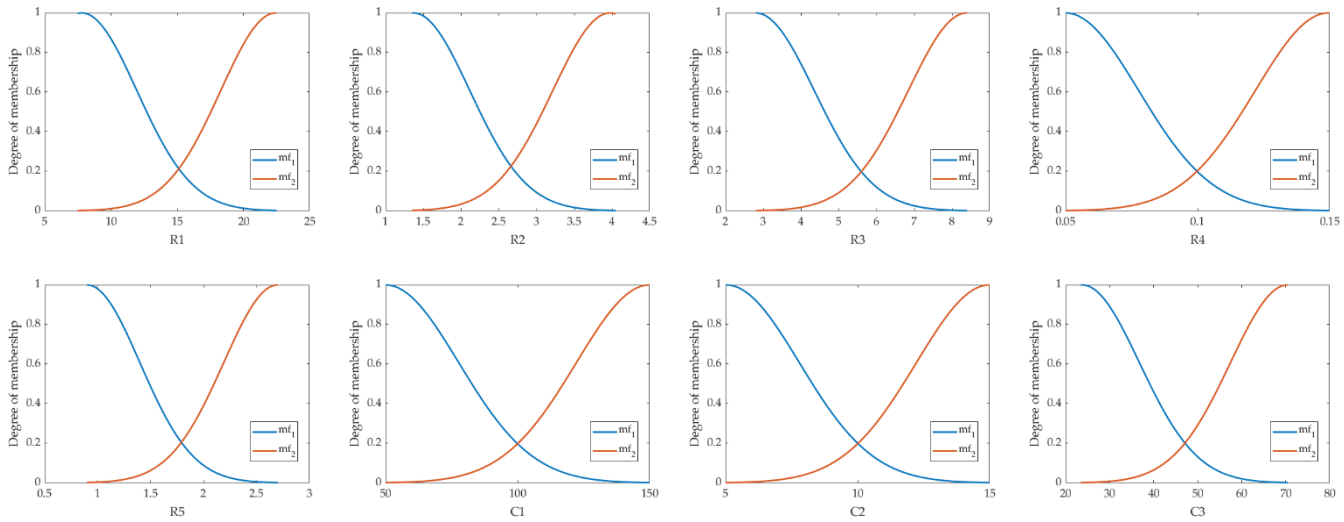

Figure 9. Membership functions obtained after tuning the FIS for THD (2nd step).

3.4. Optimization Process

Once the fuzzy inference systems were obtained, they were employed to predict the outputs and to analyze the main effects plot as well as the interaction effects plot, if necessary, so that the levels of the input variables that improve the targets (output responses) could then be selected. To verify that the new design remains stable against variations due to the tolerances of the passive elements of the circuit, a new Monte Carlo analysis was performed with the new inputs. From this analysis, the stability of the circuit could then be verified. The process can be repeated until a satisfactory result is obtained, as shown in Figure 10, which depicts a scheme of the proposed method. This optimization process is further developed in the following sections in order to improve the behavior of the electronic circuit shown in Figure 1.

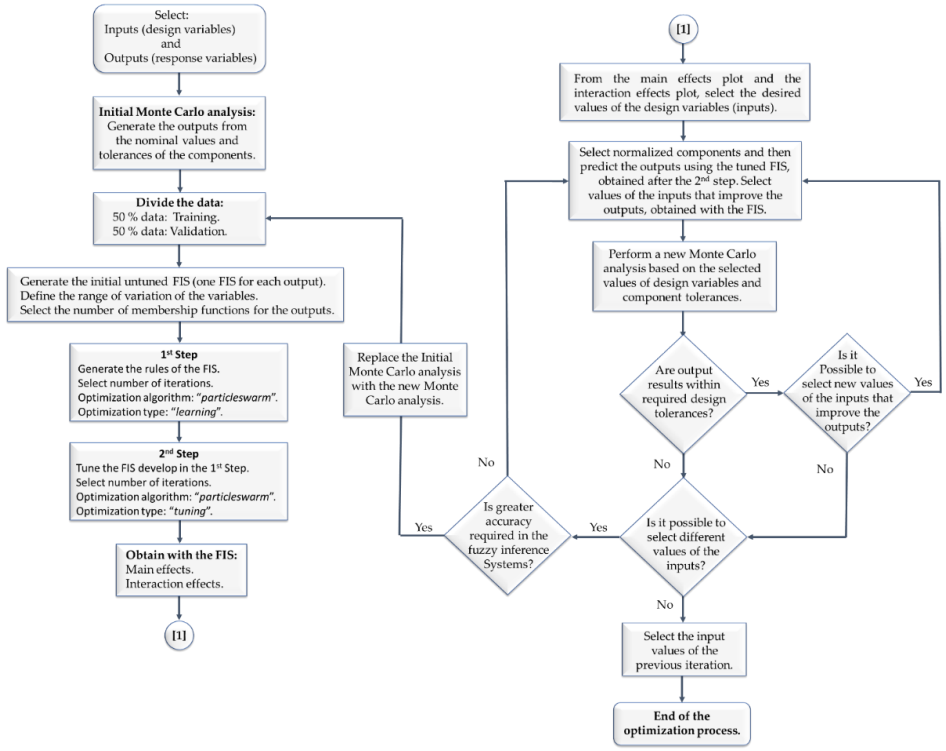

Figure 10. Scheme of the proposed method.

4. Results

The results of following the methodology described above are now presented. First, the results obtained for the voltage gain (Av) are provided, then those for the total harmonic distortion (THD).

4.1. Voltage Gain Modeling Results

Figure 11 shows the results after the first step in the development of the FIS. As can be observed, this FIS is capable of accurately modeling the voltage gain's behavior. The data shown in Tables A1 and A2 were used to obtain both the MSE and the relative error values of these results. The values in Table A1 were employed to obtain the FIS and the values in Table A2 for its validation. The accuracy of the fuzzy inference systems can be determined using either the mean squared error (MSE) or using the root mean squared error (RMSE), where y_i is the actual value and $\hat{y}_i$ is the estimated one, as shown in Equation (7).

$$MSE = \frac{1}{N}\sum_{i=1}^{N}(y_i - \hat{y}_i)^2 \qquad RMSE = \sqrt{MSE} \tag{7}$$

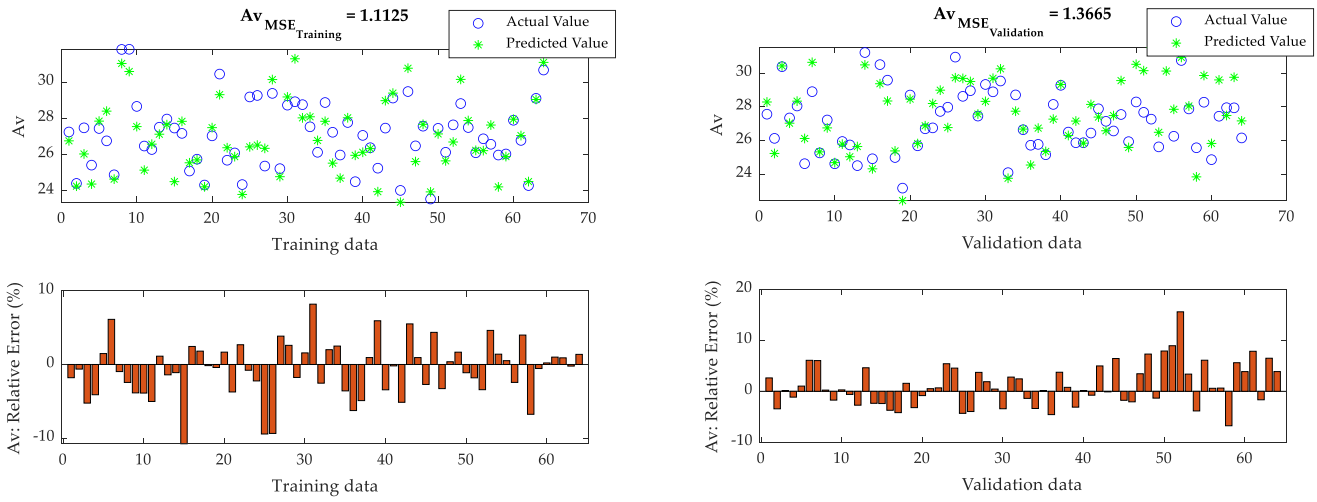

(**a**) (**b**)

Figure 11. Results with the tuned FIS in the first step for Av: (**a**) training data; (**b**) validation data.

As can be observed in Figure 12, after the second step, the results were more accurate than those obtained with the previous FIS; hence, the adjusted FIS was used to model the behavior of the circuit. Increasing the number of iterations may reduce the MSE. However, increasing the number of iterations also increases the calculation time. It was, therefore, decided to use 100 iterations for both response variables.

As can be observed in Figure 12, the FIS was capable of adequately predicting the voltage gain behavior. This model could be used to obtain both the interaction and the main effects as well as the response surfaces. Figure 13 shows the response surfaces for the voltage gain versus R_3 and {R_1, R_2, R_4, R_5, C_1, C_2, C_3}. The same could be performed for all the other input variables.

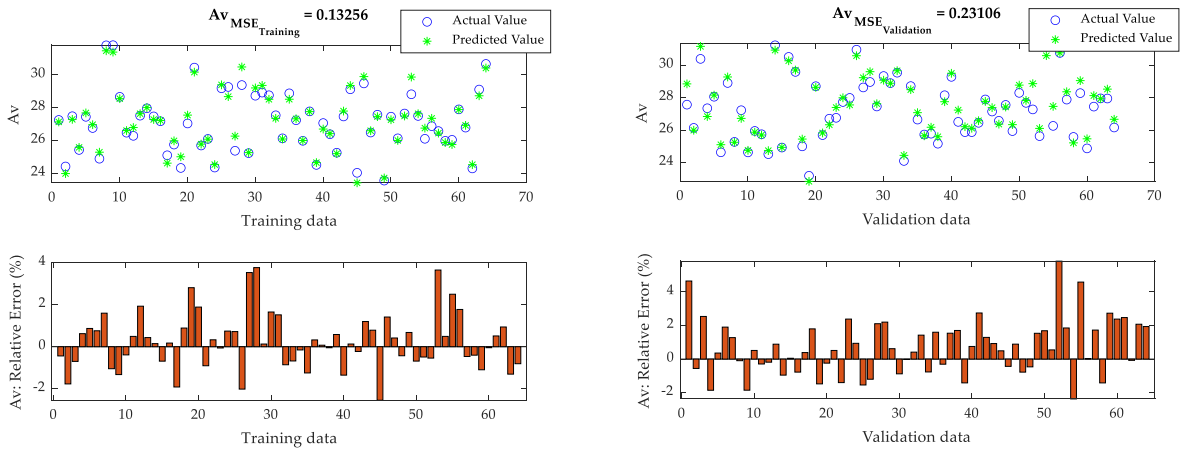

(**a**) (**b**)

Figure 12. Results obtained with the tuned FIS in the second step for Av: (**a**) training data, (**b**) validation data.

4.2. Results of Modeling Total Harmonic Distortion

Figure 14 shows the results from the first step in the development of the FIS for the THD. As in the previous case, this FIS was capable of accurately modeling the THD and, therefore, its behavior. Similarly, the data shown in Tables A1 and A2 were used to obtain both the MSE and the relative error values of these results.

The results improved after tuning the FIS, as shown in Figure 15; hence, this tuned FIS was the one employed for modeling the THD.

From this FIS obtained after the second step, both the response surfaces and the main effects as well as the interaction effects were obtained. Figure 16 shows the response surfaces for the THD versus R_1 and all the other components analyzed in this study.

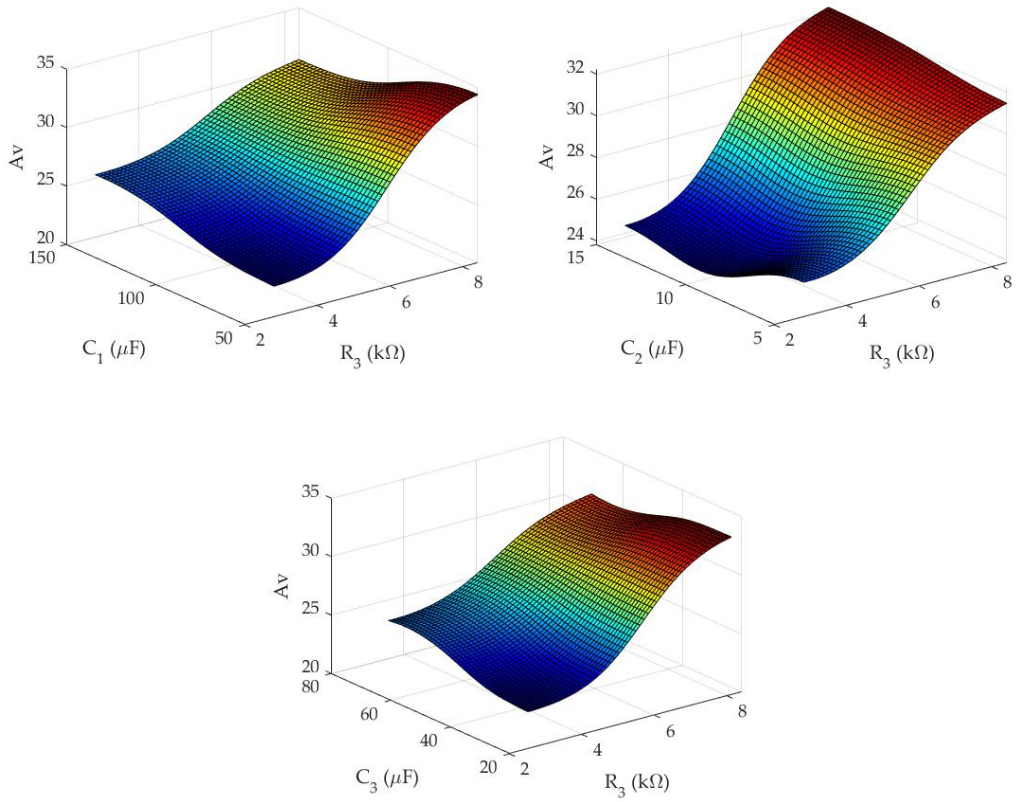

Figure 13. *Cont.*

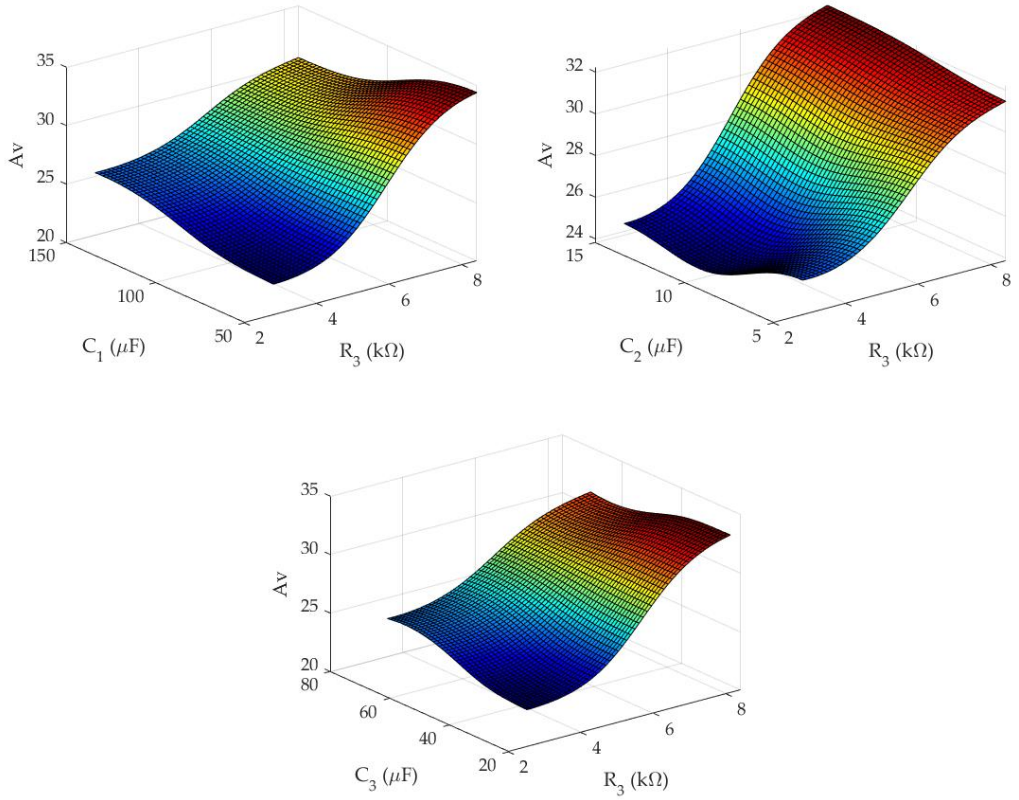

Figure 13. Response surface for Av vs. R_3 and {R_1, R_2, R_4, R_5, C_1, C_2, C_3}.

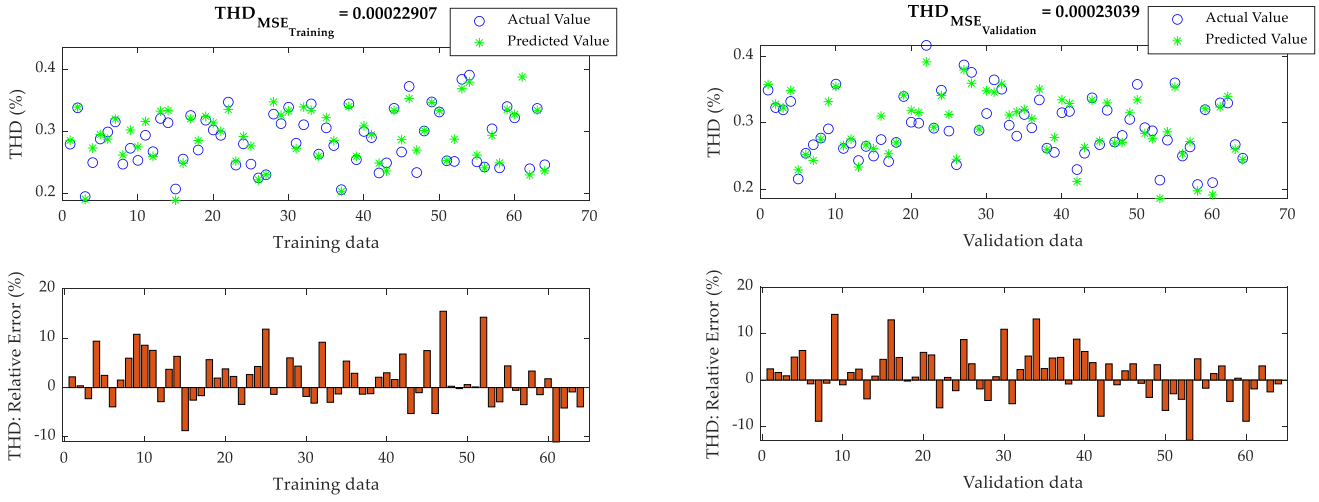

(**a**) (**b**)

Figure 14. Results of the tuned FIS in the first step for THD: (**a**) training data; (**b**) validation data.

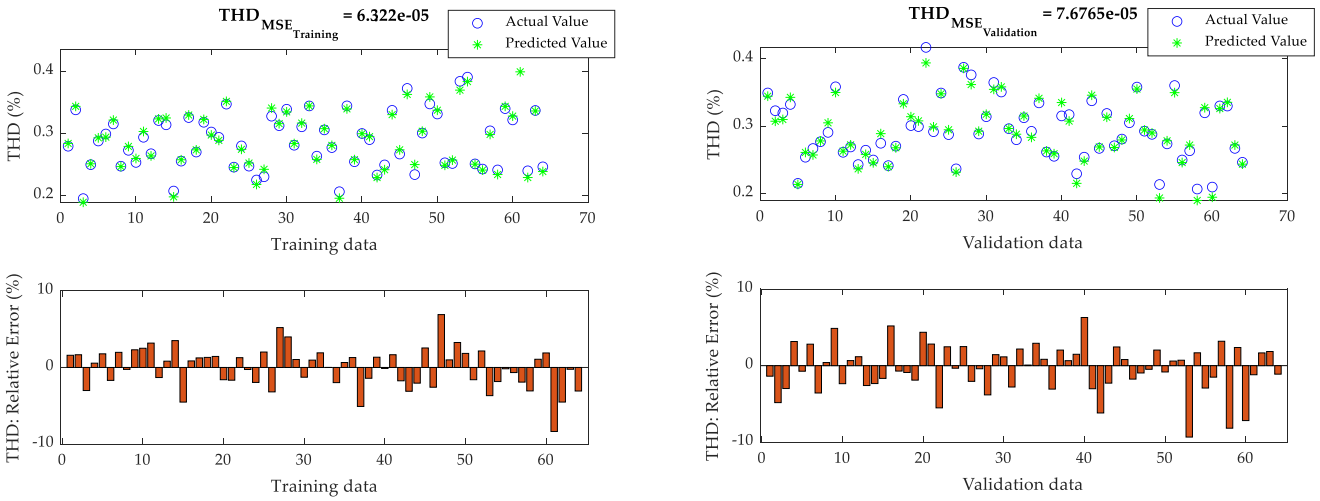

(**a**) (**b**)

Figure 15. Results of the tuned FIS in the second step for THD: (**a**) training data; (**b**) validation data.

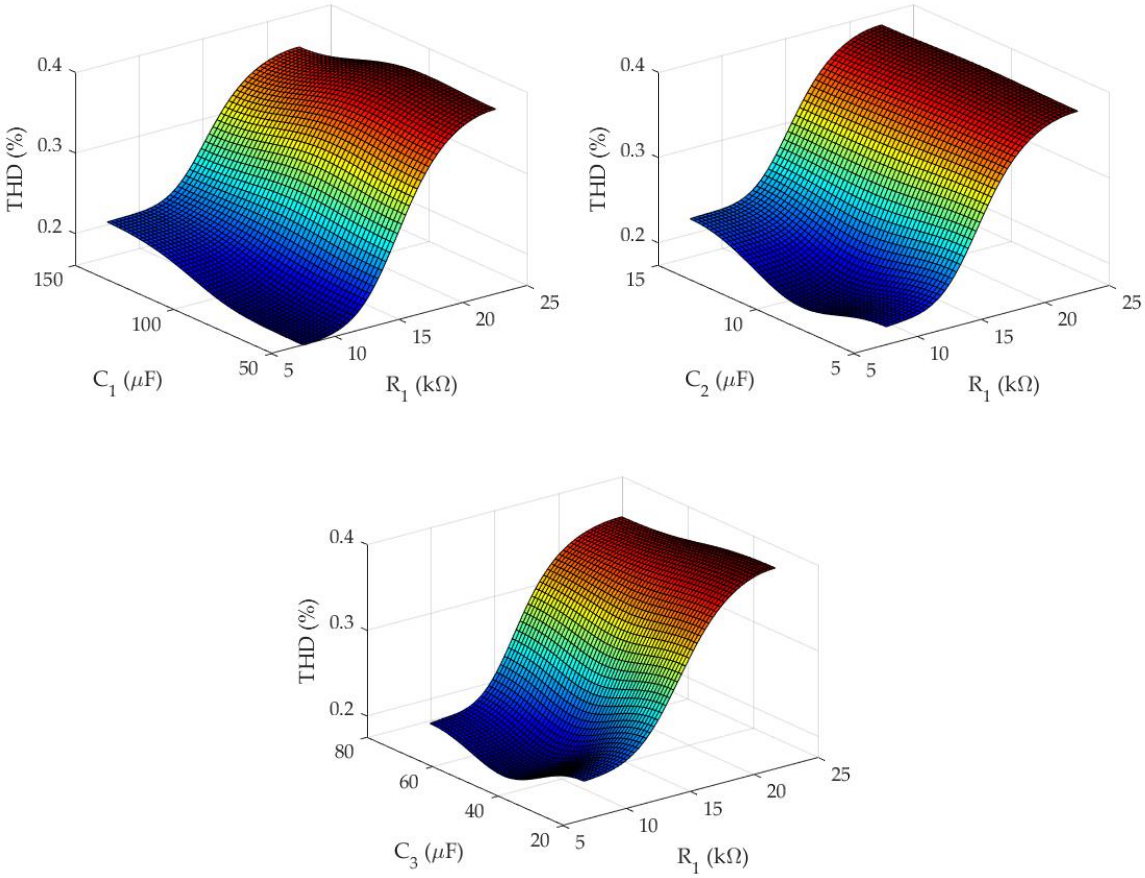

Figure 16. *Cont*.

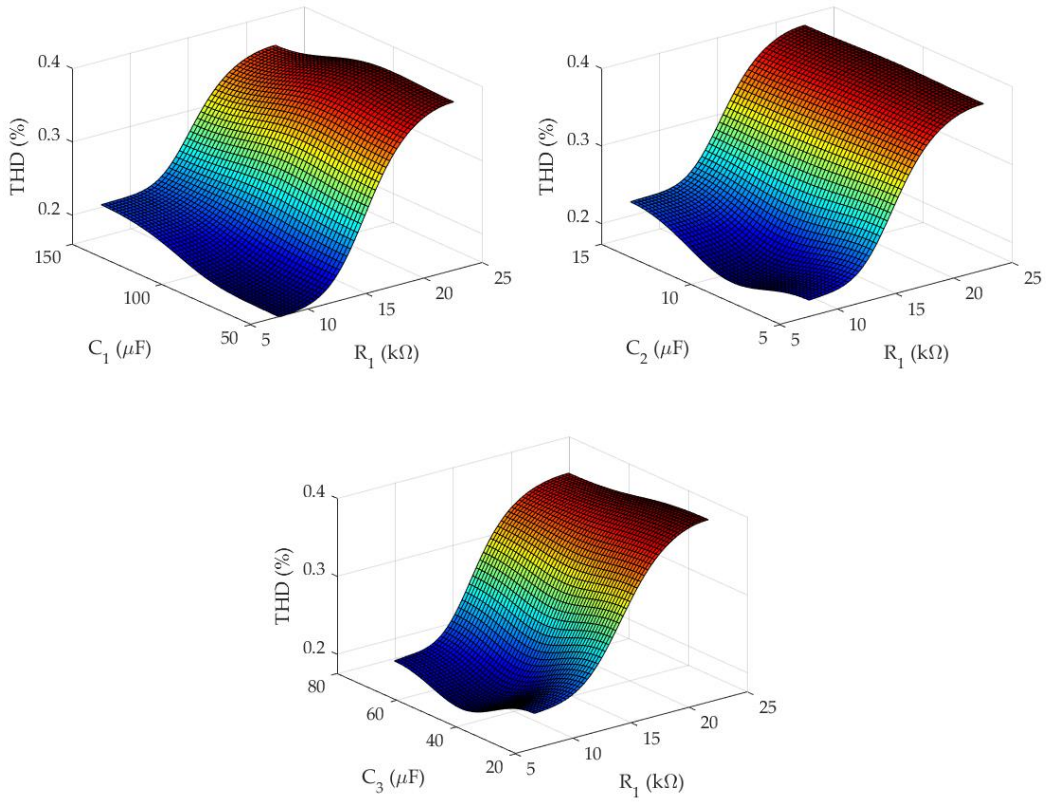

Figure 16. Response surface for THD vs. R_1 and {R_2, R_3, R_4, R_5, C_1, C_2, C_3}.

5. Discussion

In this section, the results are analyzed to show how this methodology can be used to improve an initial circuit design. Figure 17 shows the main effects plot for the Av. As can be seen from Figure 17, the variables that have the strongest influence on the voltage gain are R_3, which has a positive correlation, and R_4, which has a negative correlation with the voltage gain. Therefore, an increase in R_3 and a decrease in R_4 would increase the voltage gain of the amplifier. The rest of the parameters have less influence on the voltage gain. Figure 17 shows that the preferred variations to increase the gain voltage are that R_2 increases and R_1 and R_5 decrease. The capacitors have less influence.

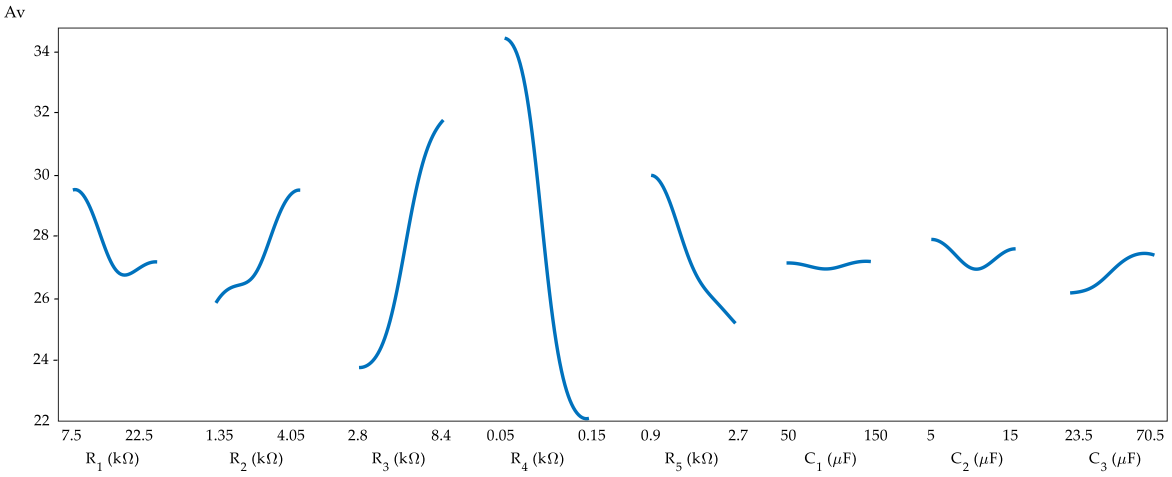

Figure 17. Main effects plot for Av using the FIS.

Regarding harmonic distortion, the behavior of R_4 is unlike that of the voltage gain, i.e., whereas the preferred variation for R_4 is to decrease, in order to increase the voltage gain, in the case of the THD, a decrease in R_4 provokes greater harmonic distortion. Therefore, a compromise between both variables should be considered.

New values for the circuit components may be selected from the results shown in the main effects plots depicted in Figures 17 and 18. However, in general, these values should be normalized values, and within the same series of tolerances. Moreover, it is possible to employ the fuzzy inference systems developed for both the Av and the THD to predict the response of the circuit. These predicted values are shown in Table 4. Therefore, in the first iteration, it was decided to increase R_3, selecting a normalized value greater than the one shown in Table 1, and to simultaneously decrease R_4 to a value lower than that shown in Table 1, adopting a normalized value as in the previous case. Therefore, the selected values in this first iteration were R_3 = 7.5 kΩ and R_4 = 0.075 kΩ, leaving the rest of the circuit components unchanged. Using the two fuzzy inference systems developed in the second step for the Av and the THD, their predicted values were Av = 35.2113 and THD = 0.3441%.

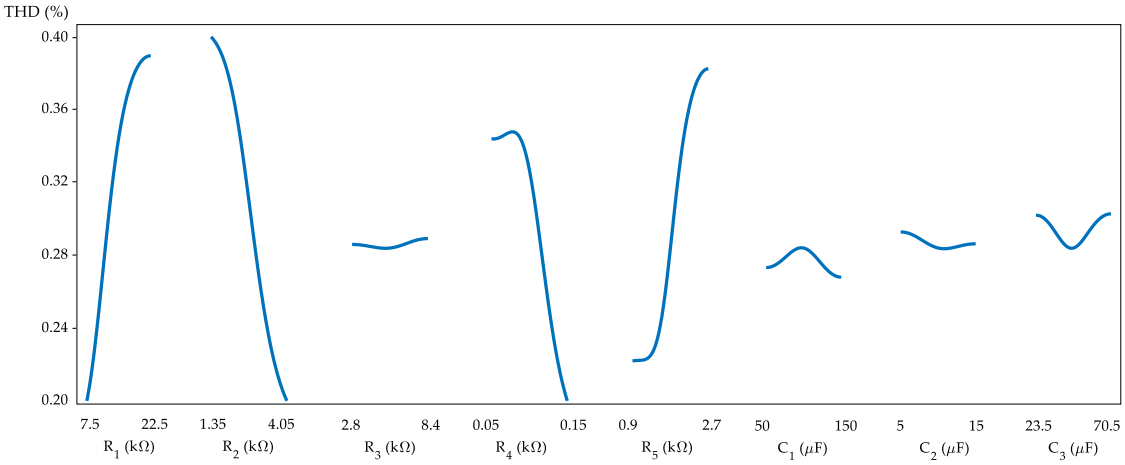

Figure 18. Main effects plot for THD using the FIS.

Table 4. Predicted values using the tuned FIS obtained for both Av and THD.

R_3 (kΩ)	R_4 (kΩ)	Av	THD
7.5	0.075	35.2113	0.3441
	0.068	35.7590	0.3424
	0.062	36.0746	0.3395
	0.056	36.3095	0.3372
8.2	0.075	35.5718	0.3434
	0.068	36.0723	0.3415
	0.062	36.3669	0.3385
	0.056	36.5998	0.3362
9.1	0.075	35.8258	0.3438
	0.068	36.2898	0.3421
	0.062	36.5649	0.3391
	0.056	36.7891	0.3368

Notably, the main effect plots shown in Figures 17 and 18 suggest an increase in the value of R_3 of over 7.5 kΩ and a decrease in the value of R_4. However, before selecting these values, the circuit stability should be confirmed with the new selected values of the

components, which is discussed below. When analyzing the response of the circuit with these new values through simulation, Av = 40.4191 and THD = 0.4140% were obtained. Both fuzzy inference systems offered an approximation of the behavior obtained through simulation, as shown in Figure 19. If the fuzzy inference systems were trained with more values than those employed in Table A1, then their precision would increase. In any case, the FIS was capable of predicting the behavior of both the Av and the THD. Figure 19 shows the initial and the optimized design after the first iteration.

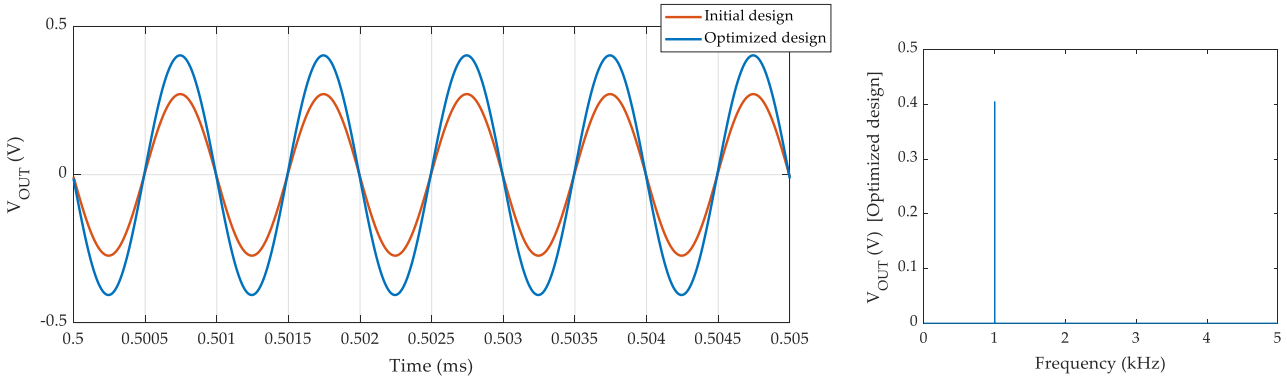

Figure 19. Comparison between the initial design and the optimized design after the first iteration.

The initial design produced the following values: Av = 27.2472 and THD = 0.2795%. If the harmonic distortion in the new design is considered acceptable, then the voltage gain improvement when R_3 = 7.5 kΩ and R_4 = 0.075 kΩ is 48%. In any case, to verify that the new design remains stable against variations in resistors and capacitors due to the tolerances of the passive elements of the circuit, a Monte Carlo analysis was conducted with the new design. The components of the circuit were varied using a uniform distribution, and the results of the voltage gain and the harmonic distortion are shown in Figure 20, respectively.

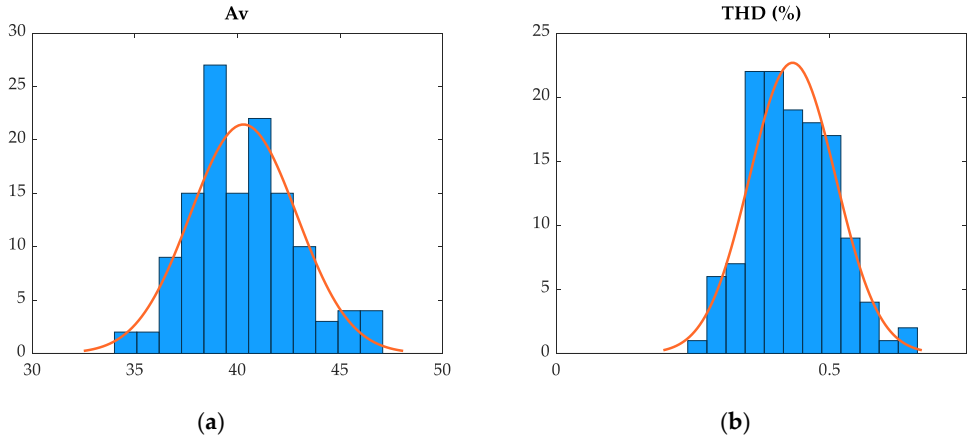

Figure 20. Histogram of (**a**) Av and (**b**) THD, when R_3 = 7.5 kΩ and R_4 = 0.075 kΩ.

Table 5 shows the average values and the standard deviation of the values shown in Figure 20. As can be observed, the circuit remains stable against variations in the circuit components due to their tolerances. Figure 21 shows the outputs of the Monte Carlo analysis.

Table 5. Average and standard deviation values obtained from the Monte Carlo analysis with the new design (R_3 = 7.5 kΩ and R_4 = 0.075 kΩ).

$\overline{Av}$	S_{Av}	$\overline{THD}$ (%)	S_{THD} (%)
40.2901	2.5959	0.4317	0.0788

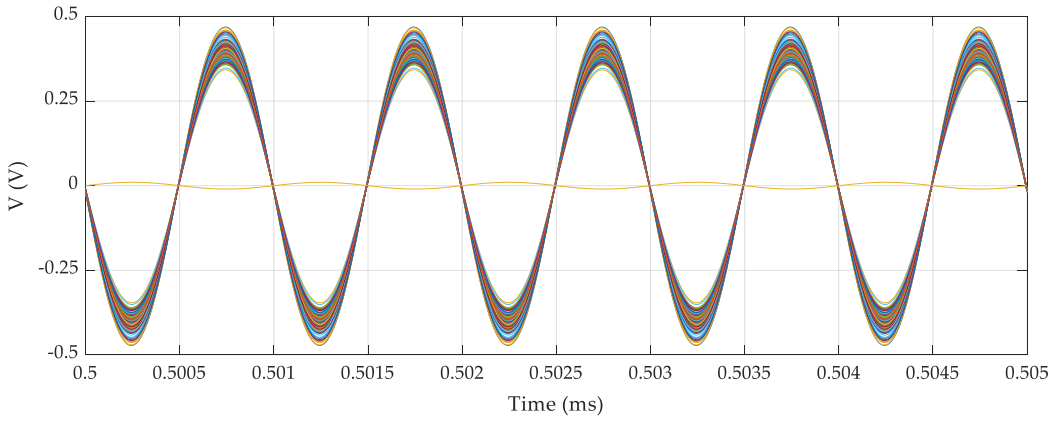

Figure 21. Response of the amplifier with R_3 = 7.5 kΩ and R_4 = 0.075 kΩ (Monte Carlo analysis).

Table 5 shows that the average value of the voltage gain increases, but the total harmonic distortion worsens. If these THD values are considered acceptable, then new values of R_3 and R_4 could be selected. In this case, from Figure 17 and Table 4, a higher value than 7.5 kΩ could have been selected.

New values were, therefore, chosen within the 10% series of tolerance (R_3 = 9.1 kΩ; R_4 = 0.056 kΩ) and the values of all the other components showed no variation with respect to the previous stage. When the new circuit was simulated, the results shown in Figure 22 were obtained, where Av = 55.46574 and THD = 0.6314%. Notably, since the new input values were outside the range of values used to train the FIS, a greater discrepancy was observed in these results with regard to the data obtained through simulation. If the fuzzy inference systems were trained with more values than those employed in Table A1, then their precision would increase. Likewise, if the values of the Monte Carlo analysis obtained with the new modified inputs were used to train the fuzzy inference systems, their precision could also be increased. However, in this study, the fuzzy inference systems developed from data shown in Table A1 were capable of predicting the output variable trends and, hence, they were not modified.

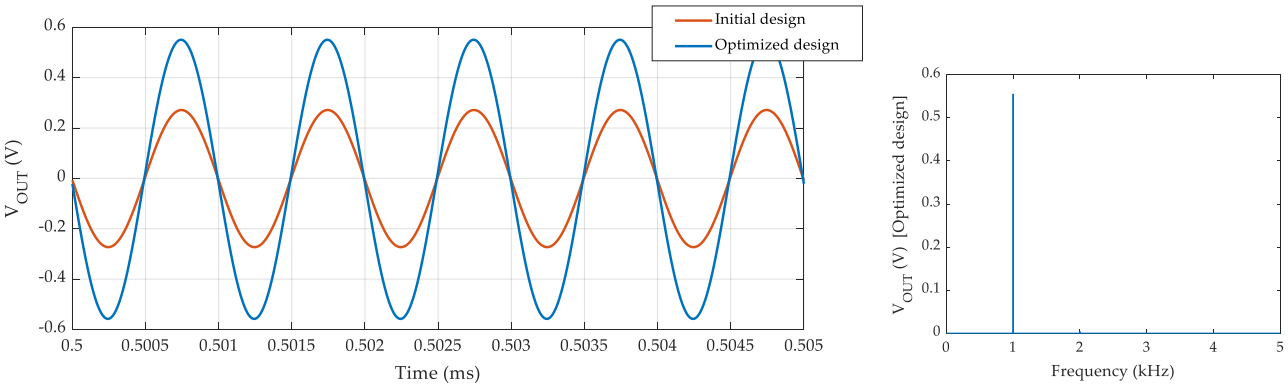

Figure 22. Comparison between the initial design and the optimized design with the second iteration.

Table 6 shows the average values and the standard deviation values following a Monte Carlo analysis of this new design. These results are shown in Figure 23.

Table 6. Average and standard deviation values obtained from the Monte Carlo analysis with the new design (R_3 = 9.1 kΩ and R_4 = 0.056 kΩ).

$\overline{Av}$	S_{Av}	$\overline{THD}$ (%)	S_{THD} (%)
55.2387	3.4490	0.6552	0.1187

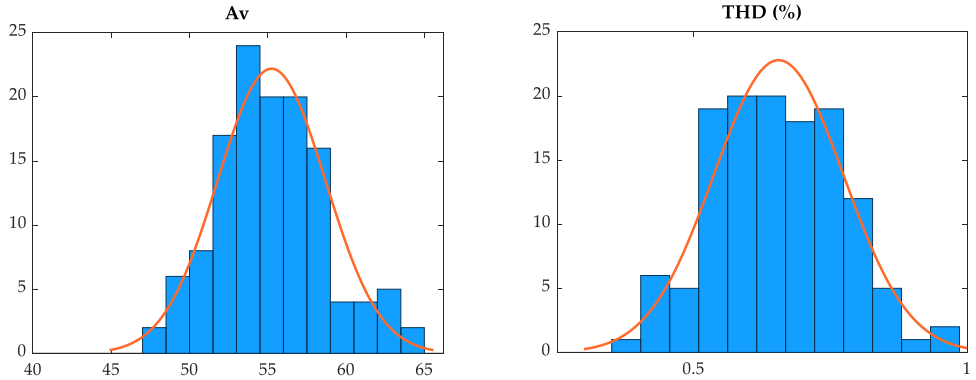

Figure 23. Histogram of (**a**) Av and (**b**) THD, when R_3 = 9.1 kΩ and R_4 = 0.056 kΩ.

Figure 24 shows the outputs obtained in the Monte Carlo Analysis. As can be observed in Figure 23, the circuit remains stable against variations in the components as a consequence of their tolerances. Moreover, with the new values obtained within the second iteration, the voltage gain increases to 104% compared to the initial circuit design.

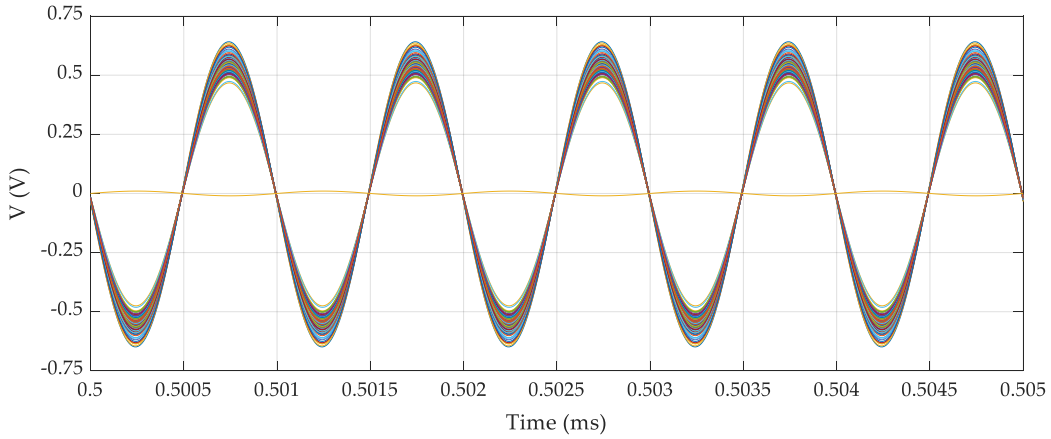

Figure 24. Response of the amplifier with R_3 = 9.1 kΩ and R_4 = 0.056 kΩ (Monte Carlo analysis).

6. Conclusions

In the present study, zero-order Sugeno fuzzy inference systems were optimized with a PSO algorithm and used to model the behavior of an electronic circuit used as a small signal amplifier.

It was shown that a Monte Carlo analysis can be combined with FIS modeling in an iterative process to optimize the design of an electronic circuit. Likewise, the stability of the optimized design and its stability against component variations due to their tolerances should be analyzed in order to select the optimized design, because independent optimizations can lead to results that are not feasible due, in general, to the selection of normalized components for building an electronic circuit.

The methodology analyzed in this study can serve as a basis for improving the design of analog electronic circuits with a similar configuration to the one that was considered in this study. Future research studies will include the application of the proposed methodology to improve the design of other types of analog electronic circuits as well as the use of different fuzzy inference systems and membership functions.

Funding: This research received no external funding.

Conflicts of Interest: The author declares no conflict of interest.

Appendix A

Table A1. Training data.

R_1 (kΩ)	R_2 (kΩ)	R_3 (kΩ)	R_4 (kΩ)	R_5 (kΩ)	C_1 (μF)	C_2 (μF)	C_3 (μF)	Av	THD (%)
15.0000	2.7000	5.6000	0.1000	1.8000	100.0000	10.0000	47.0000	27.2472	0.2795
15.8328	2.4461	5.2137	0.1044	1.8104	93.7963	10.7401	41.1585	24.4094	0.3381
13.5113	2.9661	5.8923	0.1075	1.6771	104.8370	11.4192	45.2265	27.4756	0.1951
13.5667	2.6187	5.6423	0.1093	1.9400	117.9850	8.6107	38.1179	25.4181	0.2498
15.6246	2.8114	5.5851	0.0988	1.8161	109.5620	11.6946	46.1542	27.4388	0.2879
13.7777	2.5235	5.6920	0.1020	1.9739	81.4696	11.1739	52.6052	26.7572	0.2992
16.1078	2.5339	5.2432	0.1037	1.7462	94.4325	8.0773	43.3199	24.8841	0.3154
14.7103	2.9334	6.0935	0.0913	1.6616	84.3982	8.6627	43.9616	31.8005	0.2473
13.9487	2.8300	6.0940	0.0901	1.8165	95.3202	11.0554	38.3347	31.8091	0.2729
14.6361	2.7239	5.8275	0.0986	1.6952	101.1070	10.8608	42.5919	28.6573	0.2534
15.3158	2.4830	6.0395	0.1069	1.7714	105.6460	10.1871	54.0030	26.4716	0.2939
15.8724	2.8047	5.7784	0.1063	1.8060	117.6900	8.2420	53.0132	26.2795	0.2674
15.8343	2.5230	5.6213	0.0975	1.6886	103.9810	9.9843	43.4115	27.5104	0.3209
15.4539	2.7421	5.2024	0.0918	1.7738	100.1980	10.6460	38.8507	27.9602	0.3140
14.2455	2.8414	6.1301	0.1090	1.6549	114.5590	9.0375	51.4034	27.4646	0.2073
14.6344	2.9345	5.8410	0.1041	1.9592	83.8160	8.4907	53.8347	27.1700	0.2555
15.3007	2.5382	5.0740	0.1004	1.8434	85.9512	10.8360	40.0548	25.0930	0.3257
15.0714	2.8898	5.1404	0.1010	1.8956	106.7890	10.3655	42.3755	25.7461	0.2701
15.7207	2.6150	5.0801	0.1040	1.8833	103.5130	8.0451	47.9438	24.3201	0.3181
15.0962	2.5152	5.4224	0.0979	1.7102	114.9440	11.6311	54.6840	27.0336	0.3024
14.9390	2.6867	5.9950	0.0925	1.7271	117.7940	10.3133	47.7135	30.4415	0.2938
15.2144	2.5505	5.1709	0.0984	1.9162	86.5190	9.0900	48.1769	25.6892	0.3473
14.6807	2.6672	5.5050	0.1052	1.7156	87.1537	10.5414	42.3552	26.0909	0.2458
15.0398	2.5726	5.3063	0.1085	1.8406	114.9820	10.3411	54.2173	24.3451	0.2800
13.8065	2.5064	6.0848	0.0996	1.6302	115.6490	8.2284	51.5068	29.1801	0.2474
13.5822	2.9367	6.1033	0.1007	1.8314	97.9916	8.4112	45.0181	29.2616	0.2251
15.3643	2.8067	5.4116	0.1081	1.6613	90.1408	8.0493	56.0917	25.3678	0.2303
16.2798	2.9650	5.5904	0.0907	1.8635	105.1510	11.5560	39.7557	29.3758	0.3279
15.7823	2.4571	5.1765	0.1016	1.6785	107.0250	9.8955	43.9948	25.2248	0.3126

Table A1. *Cont.*

R_1 (kΩ)	R_2 (kΩ)	R_3 (kΩ)	R_4 (kΩ)	R_5 (kΩ)	C_1 (μF)	C_2 (μF)	C_3 (μF)	Av	THD (%)
16.0049	2.5858	5.5715	0.0922	1.6908	91.8360	8.3607	43.8447	28.7273	0.3391
16.3011	2.9579	6.0432	0.0984	1.7935	98.3949	10.6177	49.4036	28.9168	0.2811
14.7704	2.6251	5.3794	0.0912	1.7530	113.3270	8.8173	40.9571	28.7548	0.3108
15.2298	2.5756	5.6520	0.0969	1.8965	86.4495	10.3353	46.5269	27.5325	0.3444
13.7578	2.6510	5.2543	0.1012	1.8727	81.1176	8.7089	45.3767	26.1262	0.2635
14.5743	2.6328	6.0512	0.0976	1.8902	113.0510	11.6165	43.5606	28.8717	0.3058
14.3022	2.6812	6.0608	0.1049	1.9635	99.2231	8.0318	47.4785	27.2309	0.2773
14.2064	2.9670	5.3386	0.1063	1.6857	119.4460	10.2803	43.0357	25.9752	0.2062
16.2513	2.6083	5.2938	0.0923	1.6980	94.7161	8.5510	38.4080	27.7704	0.3445
14.1435	2.5163	5.0741	0.1061	1.7392	80.1077	11.0453	42.3184	24.5048	0.2545
15.8654	2.6773	6.0979	0.1049	1.8506	117.3400	11.2663	44.0902	27.0581	0.3000
15.1557	2.6751	5.0457	0.0965	1.7452	95.2587	9.5726	43.0080	26.3787	0.2901
14.2538	2.5841	5.5324	0.1098	1.6981	119.2280	9.1884	41.2814	25.2497	0.2331
14.6398	2.8552	5.2098	0.0964	1.7233	89.1312	10.8486	48.7945	27.4615	0.2494
15.6254	2.6288	5.7272	0.0925	1.7729	84.0560	11.0075	37.6818	29.1186	0.3373
14.8994	2.5367	5.1323	0.1084	1.7570	102.2310	10.6577	40.3564	24.0232	0.2669
16.2192	2.7192	6.1004	0.0935	1.9193	112.3190	9.0792	54.8405	29.4774	0.3726
14.5600	2.8285	5.1974	0.1007	1.6900	115.0370	11.3368	41.3772	26.4811	0.2338
14.9926	2.6836	6.1360	0.1033	1.9540	95.8820	10.8216	49.7218	27.5677	0.3007
16.4550	2.4583	5.1632	0.1073	1.8205	89.4335	10.4993	51.2953	23.5491	0.3476
16.2926	2.7946	5.5193	0.0963	1.8644	91.4236	8.6989	40.8575	27.4479	0.3314
14.2472	2.7253	5.2875	0.1021	1.8111	97.2083	9.8529	46.2522	26.1261	0.2528
13.7003	2.5381	5.6128	0.1001	1.7033	102.5320	8.4922	38.2658	27.6396	0.2517
16.3455	2.4376	5.8567	0.0931	1.6943	100.9120	9.2021	53.8982	28.8142	0.3840
15.7471	2.6377	5.4115	0.0929	1.9681	104.8980	8.8470	43.3563	27.4928	0.3908
14.6554	2.5783	5.8442	0.1087	1.7343	83.4408	10.1864	41.2969	26.0993	0.2510
15.2204	2.7875	6.1411	0.1090	1.7750	84.1386	9.0668	44.6015	26.8714	0.2427
14.3042	2.6271	5.5371	0.1008	1.9799	82.8850	11.0893	45.5187	26.5682	0.3043
13.8151	2.7067	5.7973	0.1092	1.9058	119.0810	8.5519	40.5689	25.9746	0.2413
16.3724	2.6989	5.4364	0.1003	1.8898	94.8602	10.3207	43.4029	26.0339	0.3401
14.8373	2.5930	5.7323	0.0973	1.8845	98.5751	10.0196	49.6320	27.8934	0.3219
16.1613	2.4699	5.1471	0.0911	1.8672	103.1570	11.8951	38.5787	26.7814	0.4358
13.7713	2.7065	5.1507	0.1089	1.8993	96.8691	10.1285	54.7968	24.2918	0.2399
15.5724	2.7966	5.5642	0.0910	1.8802	89.8738	9.9117	40.7387	29.1027	0.3371
14.1829	2.9065	6.1304	0.0951	1.7792	92.9172	10.8046	49.3129	30.6644	0.2463

Table A2. Validation data.

R_1 (kΩ)	R_2 (kΩ)	R_3 (kΩ)	R_4 (kΩ)	R_5 (kΩ)	C_1 (μF)	C_2 (μF)	C_3 (μF)	Av	THD (%)
14.5830	2.5653	5.2105	0.0920	1.9019	112.9760	8.7314	46.4496	27.5647	0.3492
14.5762	2.5057	5.6719	0.1032	1.9664	118.6260	10.7263	48.6201	26.1313	0.3229
15.5220	2.6029	6.0833	0.0924	1.6968	81.9079	10.6628	40.9475	30.3857	0.3195
16.3665	2.7102	5.7618	0.0991	1.8432	108.2710	8.4483	39.2409	27.3420	0.3322
13.6689	2.8323	5.4870	0.0994	1.6436	84.2440	8.6486	37.8405	28.0525	0.2153
15.4722	2.7715	5.3851	0.1095	1.8090	87.6366	9.7989	55.9535	24.6272	0.2540
15.7550	2.8700	5.3963	0.0927	1.6257	80.2045	10.1579	48.3160	28.9021	0.2669
15.8420	2.8237	5.2071	0.1034	1.8241	94.2052	10.3729	45.2960	25.2679	0.2770
14.5129	2.5034	5.2634	0.0959	1.6959	115.0950	10.5087	38.1426	27.2210	0.2908
16.3337	2.5749	5.2371	0.1030	1.9094	112.7080	8.9622	45.8260	24.6225	0.3583
16.0079	2.8929	5.4458	0.1042	1.7805	90.2485	11.0945	42.0101	25.9433	0.2613
15.6450	2.6723	5.5283	0.1056	1.7341	102.4910	10.8223	46.2459	25.7400	0.2692
14.4381	2.7022	5.1822	0.1082	1.8037	82.2835	11.4681	49.4026	24.5134	0.2431
13.7587	2.7400	6.0640	0.0920	1.7689	91.0642	9.5492	47.5259	31.2241	0.2644
14.4409	2.8430	5.0930	0.1048	1.8968	107.5260	9.4664	41.7981	24.9196	0.2499
13.8957	2.8239	6.0666	0.0937	1.9059	117.3830	11.8247	41.0389	30.5063	0.2747
13.6292	2.6823	5.7443	0.0952	1.6735	108.6800	8.9931	49.2833	29.5840	0.2416
16.4771	2.9402	5.1946	0.1047	1.8120	113.4360	9.7881	43.8172	24.9936	0.2704
15.6344	2.4913	5.0886	0.1083	1.9602	108.0880	10.9532	47.3379	23.1779	0.3396
15.7949	2.9348	6.0369	0.0982	1.9376	115.1050	10.8535	40.8005	28.7021	0.3009
14.1614	2.4553	5.4618	0.1036	1.8862	88.8795	8.7795	37.9311	25.6882	0.2994
16.0440	2.4329	5.7732	0.0985	1.9424	106.1400	9.2498	41.6655	26.6989	0.4167
14.8907	2.8115	5.3217	0.0983	1.9303	97.3161	8.8981	50.9706	26.7532	0.2918
16.0656	2.7854	5.5507	0.0949	1.9340	99.8714	11.7586	44.7560	27.7289	0.3491
15.0012	2.6827	5.8624	0.0997	1.8195	116.1700	10.7747	40.5063	27.9791	0.2875
13.5010	2.7919	5.9039	0.0927	1.6862	104.1260	10.0354	47.0376	30.9525	0.2368
15.7953	2.4635	6.0140	0.0951	1.8376	92.5720	9.0350	52.4915	28.6252	0.3872
14.3456	2.4463	5.7082	0.0915	1.9279	88.1946	8.0742	44.6833	28.9604	0.3760
15.7035	2.7338	5.6294	0.0992	1.7569	105.1160	9.7471	48.2751	27.4526	0.2884
13.5343	2.4559	5.7377	0.0928	1.8451	111.4000	9.6311	39.0094	29.3284	0.3140
14.4324	2.5574	5.5938	0.0910	1.9598	89.8971	9.6575	47.1800	28.8919	0.3647
16.3299	2.8466	5.7083	0.0905	1.8586	114.4570	8.8412	42.9537	29.5349	0.3506
16.1163	2.4982	5.2703	0.1084	1.7077	112.5900	10.3943	52.2739	24.0953	0.2963
13.5639	2.5310	5.6301	0.0952	1.7838	108.2930	10.8274	39.2544	28.7084	0.2799
16.3197	2.5518	5.8118	0.1031	1.7113	107.0820	11.7646	49.3909	26.6445	0.3125
14.3831	2.4746	5.5833	0.1052	1.8625	115.4490	11.2968	49.9789	25.7227	0.2924
16.1349	2.4712	6.1251	0.1089	1.8557	104.9370	8.0861	39.6856	25.7746	0.3345
15.3149	2.6612	5.1756	0.1042	1.7051	81.5200	8.1517	44.5653	25.1585	0.2617
13.5772	2.7712	5.9244	0.1012	1.9484	105.1180	11.2070	38.1219	28.1449	0.2554

Table A2. *Cont.*

R_1 (kΩ)	R_2 (kΩ)	R_3 (kΩ)	R_4 (kΩ)	R_5 (kΩ)	C_1 (μF)	C_2 (μF)	C_3 (μF)	Av	THD (%)
14.9887	2.5067	6.0730	0.0960	1.7407	95.7862	9.9101	55.1282	29.2788	0.3152
16.2503	2.4384	5.7329	0.1026	1.6368	115.0820	8.8989	46.9755	26.5027	0.3171
14.2112	2.8155	5.4324	0.1062	1.7898	83.1583	11.4064	49.9944	25.8709	0.2295
13.7020	2.8071	5.2872	0.1031	1.9794	113.9190	10.8332	44.2548	25.8721	0.2541
15.4709	2.6615	5.5257	0.0998	1.9648	91.4941	9.9948	53.5010	26.4449	0.3376
15.4551	2.8216	6.0301	0.1026	1.8080	114.1990	11.9712	46.5015	27.8850	0.2671
15.6569	2.5140	5.6101	0.0988	1.7196	115.2200	9.2177	46.2895	27.1416	0.3188
15.2764	2.9333	5.7706	0.1048	1.9789	87.8616	11.8665	42.8929	26.5692	0.2710
14.0559	2.6421	5.4518	0.0973	1.8446	82.3457	11.0164	54.1351	27.5477	0.2809
15.5795	2.5093	5.2058	0.0995	1.6806	101.5820	9.0039	46.0912	25.9357	0.3051
15.8660	2.4360	5.3694	0.0909	1.6304	85.6337	10.3897	54.1901	28.2909	0.3579
14.9626	2.7714	5.5419	0.0973	1.8722	89.8643	11.1341	53.6952	27.6755	0.2926
15.3179	2.9697	5.0518	0.0935	1.8695	99.8630	10.3183	52.7786	27.2710	0.2879
13.8320	2.9283	5.4103	0.1081	1.8146	102.9100	11.5123	54.4425	25.6254	0.2136
14.6532	2.9611	6.1393	0.0919	1.8515	86.9825	8.6429	43.6974	31.3287	0.2738
16.0777	2.5879	5.3432	0.0977	1.8642	111.2320	8.7228	51.9012	26.2550	0.3602
13.8115	2.7656	5.8108	0.0918	1.6938	95.5306	11.9007	46.8936	30.7537	0.2499
14.0498	2.7342	5.7014	0.0996	1.8628	97.6366	8.3895	53.7431	27.8770	0.2636
14.1442	2.8739	5.4731	0.1096	1.6940	103.1750	9.4001	40.7142	25.5722	0.2069
15.9939	2.6618	5.7688	0.0964	1.7541	105.4650	8.9508	54.4641	28.2749	0.3198
14.6740	2.9035	5.2402	0.1096	1.6719	84.1038	11.3189	48.7921	24.8678	0.2098
14.6784	2.5717	5.0884	0.0917	1.8122	99.5354	11.7050	55.6856	27.4442	0.3300
15.2084	2.6267	5.7218	0.0966	1.8797	107.4170	9.2267	45.7707	27.9508	0.3298
15.8397	2.8798	5.5589	0.0976	1.7114	89.3589	8.8977	50.1833	27.9429	0.2671
15.3885	2.9673	5.3268	0.1028	1.7962	99.5831	11.9620	46.6570	26.1563	0.2465

References

1. Mamdani, E.H. Application of fuzzy algorithms for control of simple dynamic plant. *Proc. Inst. Electr. Eng.* **1974**, *121*, 1585–1588. [CrossRef]
2. Takagi, T.; Sugeno, M. Fuzzy identification of systems and its applications to modeling and control. *IEEE Trans. Syst. Man. Cybern.* **1985**, *SMC-15*, 116–132. [CrossRef]
3. Kar, S.; Das, S.; Ghosh, P.K. Applications of neuro fuzzy systems: A brief review and future outline. *Appl. Soft Comput.* **2014**, *15*, 243–259. [CrossRef]
4. Precup, R.-E.; Hellendoorn, H. A survey on industrial applications of fuzzy control. *Comput. Ind.* **2011**, *62*, 213–226. [CrossRef]
5. Oltean, G.; Miron, C.; Zahan, S.; Gordan, M. A fuzzy optimization method for CMOS operational amplifier design. In Proceedings of the 5th Seminar on Neural Network Applications in Electrical Engineering. NEUREL 2000 (IEEE Cat. No.00EX287), Belgrade, Serbia, 25–27 September 2000; pp. 152–157. [CrossRef]
6. Sahu, B.; Dutta, A.K. A fuzzy logic based approach for parametric optimization of MOS operational amplifiers. *Microelectronics J.* **2002**, *33*, 253–264. [CrossRef]
7. Hayati, M.; Rezaei, A.; Seifi, M.; Naderi, A. Modeling and simulation of combinational CMOS logic circuits by ANFIS. *Microelectronics J.* **2010**, *41*, 381–387. [CrossRef]
8. Hostos, H.; Sanabria, F.; Melgarejo, M. Analog circuit design using genetic algorithms with fuzzy fitness function. In Proceedings of the 2010 IEEE ANDESCON, Bogotá, Columbia, 14–17 September 2010; pp. 1–5. [CrossRef]
9. Wang, X.; Zhou, C.; Zhang, Z.; Ren, T.; Liu, L. Optimal RF IC design based on Fuzzy Genetic Algorithm. In Proceedings of the 2009 Asia Pacific Conference on Postgraduate Research in Microelectronics & Electronics (PrimeAsia), Shanghai, China, 19–21 November 2009; pp. 229–232. [CrossRef]

10. Chang, G.W.; Shih, T.Y.; Chuang, G.S.; Chu, S.Y. A Fuzzy Approach for Placement of Capacitors with Considering Harmonic Distortions. In Proceedings of the 2007 International Conference on Intelligent Systems Applications to Power Systems, Washington, DC, USA, 2–5 November 2007; pp. 1–5. [CrossRef]
11. Panoiu, M.; Panoiu, C.; Ghiormez, L. Neuro-fuzzy modeling and prediction of current total harmonic distortion for high power nonlinear loads. In Proceedings of the 2018 Innovations in Intelligent Systems and Applications (INISTA), Thessaloniki, Greece, 3–5 July 2018; pp. 1–7. [CrossRef]
12. Arabi, A.; Bourouba, N.; Belaout, A.; Ayad, M. An accurate classifier based on adaptive neuro-fuzzy and features selection techniques for fault classification in analog circuits. *Integration* **2019**, *64*, 50–59. [CrossRef]
13. El-Gamal, M.A.; Abdulghafour, M. Fault isolation in analog circuits using a fuzzy inference system. *Comput. Electr. Eng.* **2003**, *29*, 213–229. [CrossRef]
14. Kavithamani, A.; Manikandan, V.; Devarajan, N. Analog circuit fault diagnosis based on bandwidth and fuzzy classifier. In Proceedings of the TENCON 2009-2009 IEEE Region 10 Conference, Singapore, 23–26 November 2009; pp. 1–6. [CrossRef]
15. Ram, R.B.; Moorthy, V.P.; Devarajan, N. Fuzzy based time domain analysis approach for fault diagnosis of analog electronic circuits. In Proceedings of the 2009 International Conference on Control, Automation, Communication and Energy Conservation, Erode, India, 4–6 June 2009; pp. 1–6.
16. Calcagno, S.; Morabito, F.C.; Versaci, M. A novel approach for detecting and classifying defects in metallic plates. *IEEE Trans. Magn.* **2003**, *39*, 1531–1534. [CrossRef]
17. Guo, C.; Zhang, L.; Qian, Y.; Huang, C.; Wang, H.; Yao, L.; Jiang, X. Application of adaptive neuro fuzzy inference system to the partial discharge pattern recognition. In Proceedings of the 2009 IEEE International Conference on Intelligent Computing and Intelligent Systems, Shanghai, China, 20–22 November 2009; pp. 729–732. [CrossRef]
18. Voloşencu, C. Stability analysis of systems with fuzzy pi controllers applied to electric drives. *Mathematics* **2021**, *9*, 1246. [CrossRef]
19. Napole, C.; Barambones, O.; Calvo, I.; Derbeli, M.; Silaa, M.Y.; Velasco, J. Advances in Tracking Control for Piezoelectric Actuators Using Fuzzy Logic and Hammerstein-Wiener Compensation. *Mathematics* **2020**, *8*, 2071. [CrossRef]
20. Eboule, P.S.P.; Pretorius, J.H.C.; Mbuli, N. Artificial Neural Network Techniques apply for Fault detecting and Locating in Overhead Power Transmission Line. In Proceedings of the 2018 Australasian Universities Power Engineering Conference (AUPEC), Auckland, New Zealand, 27–30 November 2018; pp. 1–6. [CrossRef]
21. Alhato, M.M.; Ibrahim, M.N.; Rezk, H.; Bouallègue, S. An enhanced dc-link voltage response for wind-driven doubly fed induction generator using adaptive fuzzy extended state observer and sliding mode control. *Mathematics* **2021**, *9*, 963. [CrossRef]
22. Bagua, H.; Guemana, M.; Hafaifa, A.; Chaibet, A. Gas Turbine Monitoring using Fuzzy Control approaches: Comparison between Fuzzy Type 1 and 2. In Proceedings of the 2018 International Conference on Applied Smart Systems (ICASS), Médéa, Algeria, 24–25 November 2018; pp. 1–6. [CrossRef]
23. Angiulli, G.; Versaci, M. Resonant frequency evaluation of microstrip antennas using a neural-fuzzy approach. *IEEE Trans. Magn.* **2003**, *39*, 1333–1336. [CrossRef]
24. Belaout, A.; Krim, F.; Mellit, A. Neuro-fuzzy classifier for fault detection and classification in photovoltaic module. In Proceedings of the 2016 8th International Conference on Modelling, Identification and Control (ICMIC), Algiers, Algeria, 15–17 November 2016; pp. 144–149. [CrossRef]
25. Bendary, A.F.; Abdelaziz, A.Y.; Ismail, M.M.; Mahmoud, K.; Lehtonen, M.; Darwish, M.M.F. Proposed anfis based approach for fault tracking, detection, clearing and rearrangement for photovoltaic system. *Sensors* **2021**, 21. [CrossRef]
26. Chang, Y.J.; Chen, Y.M.; Lee, C.A.; Wang, Y.H.; Chen, Y.C.; Wang, C.H. Improving temperature control of laser module using fuzzy logic theory. In Proceedings of the Twentieth Annual IEEE Semiconductor Thermal Measurement and Management Symposium (IEEE Cat. No.04CH37545), Dallas, TX, USA, 14–16 March 2006; pp. 198–204. [CrossRef]
27. The MathWorks Inc. *Fuzzy Logic ToolboxTM User's Guide © Copyright 1995–2020*; The MathWorks, Inc.: Natick, MA, USA, 2020.
28. The MathWorks Inc. *Global Optimization ToolboxTM User's Guide ©Copyright 2004–2020*; The MathWorks, Inc.: Natick, MA, USA, 2020.
29. Kennedy, J.; Eberhart, R. Particle swarm optimization. In Proceedings of the ICNN'95—International Conference on Neural Networks, Perth, WA, Australia, 27 November–1 December 1995; pp. 1942–1948. [CrossRef]
30. Mezura-Montes, E.; Coello, C.A.C. Constraint-handling in nature-inspired numerical optimization: Past, present and future. *Swarm Evol. Comput.* **2011**, *1*, 173–194. [CrossRef]
31. Pedersen, M.E. Good parameters for particle swarm optimization. Tech. Rep. HL1001, Hvass Lab. HL1001, pp. 1–12, 2010. Available online: https://github.com/Hvass-Labs/Optimization-Papers/blob/main/pedersen2010good-pso-parameters.pdf (accessed on 3 September 2021).
32. Cacciola, M.; Calcagno, S.; Morabito, F.C.; Versaci, M. Swarm Optimization for Imaging of Corrosion by Impedance Measurements in Eddy Current Test. *IEEE Trans. Magn.* **2007**, *43*, 1853–1856. [CrossRef]
33. Hardt, M.; Jayaramaiah, D.; Bergs, T. On the Application of the Particle Swarm Optimization to the Inverse Determination of Material Model Parameters for Cutting Simulations. *Modelling* **2021**, *2*, 129–148. [CrossRef]
34. Liu, B.; Yuan, P.; Wang, M.; Bi, C.; Liu, C.; Li, X. Optimal Design of High-Voltage Disconnecting Switch Drive System Based on ADAMS and Particle Swarm Optimization Algorithm. *Mathematics* **2021**, *9*, 1049. [CrossRef]